Mon. Not. R. Astron. Soc. **000**, 000–000 (0000) Printed 6 December 2011 (MN LaTeX style file v2.2)

arXiv:1112.0728v1 [astro-ph.CO] 4 Dec 2011

Constraining Thawing Dark Energy using Galaxy Cluster Number Counts

N. Chandrachani Devi[1]⋆, T. Roy Choudhury[2]†, and Anjan A Sen[1]‡
[1] *Center For Theoretical Physics, Jamia Millia Islamia, New Delhi 110025, India*
[2] *Harish-Chandra Research Institute, Chhatnag Road, Jhusi, Allahabad 211019, India*

6 December 2011

ABSTRACT

We study the formation of galaxy clusters in the presence of thawing class of scalar field dark energy. We consider cases where the scalar field has canonical as well non canonical kinetic term in its action. We also consider various forms for the potential of the scalar field e.g, linear, quadratic, inverse quadratic, exponential as well as Pseudo-Nambu-Goldstone Boson (PNGB) type. Moreover we investigate situtaion where dark energy is homogeneous as well as situation where dark energy takes part in the virialization process. We use the Sheth-Torman formalism while calculating the number density of galaxy clusters. Our results show that cluster number density for different dark energy models have significant deviation from the corresponding value for the ΛCDM case. The deviation is more for higher redshifts. Moreover the tachyon type scalar field with linear potential has the highest deviation from the ΛCDM case. For the total cluster number counts, different dark energy models can have substantial deviation from ΛCDM and this deviation is most significant around $z \sim 0.5 \sim 1$ for all the models we considered.

Key words: Cosmology: Dark Energy, Thawing Model, Halos mass Function, Sheth-Torman formalism.

1 INTRODUCTION

Over the last decade, the observational data from Supernovae Type Ia(SNIa) (Kowalski et al. 2008; Riess et al. 2009), Cosmic Microwave Background (CMB)(Komatsu et al. 2011), Baryon Acoustic Oscillations (BAO)(Percival et al. 2009) and the large scale structure surveys (Cole et al. 2005) have confirmed that our Universe at present is going through an accelerated expanding phase. Till date, there has been a large number of proposals to explain such an accelerated expansion. This includes the inclusion of an unknown homogeneous matter component having a large negative pressure (cosmological constant being the simplest example of such fluid), modification of gravity of large scale as well as considering the backreaction of small scale inhomogeneities in the matter distribution.

Although inclusion of cosmological constant in the energy budget of the universe is a minimal way to explain the late time cosmological acceleration and also allowed by all cosmological observations, it is plagued by the fine tuning as well as the cosmic coincidence problems (Carroll 2001). Scalar field models with generic features can alleviate these problems and provide an alternative to cosmological constant. These dynamical scalar field models of dark energy are broadly classified into two categories-fast roll and slow roll models dubbed freezing and thawing models. For details, see the reference (Caldwell & Linder 2005). Among these, thawing scalar field models are particularly interesting as they can naturally mimic equation of state very close to $w \sim -1$ which is preferred by all the observational data.

On the other hand, information about the abundance of collapsed structures as a function of mass and redshift is an important tool to study the matter distribution in the universe (Evrard et al. 2002). A large number of cluster surveys are ongoing or being planned to be setup in near future, e.g., PLANCK, eROSITA, WFXT which would detect a large number of clusters (Vikhlinin et al. 2009b). Indeed, the mass functions of galaxy clusters have been measured through X-ray surveys (Borgani et al. 2001; Reiprich & Bohringer 2002; Vikhlinin et al. 2009a), via weak and strong lensing studies (Bartelmann et al.

⋆ E-mail:chandrachani@gmail.com
† E-mail: tirth@hri.res.in
‡ E-mail:aasen@jmi.ac.in

© 0000 RAS

1998; Dahle 2006; Corless & King 2009), using optical surveys, like the SDSS (Bahcall et al. 2003; Wen 2010) as well as through Sunayev-Zeldovich effect (Tauber 2005). In the last decade several authors have been involved in such studies and have found that the dark energy not only affects the expansion rate of the background and the distance-redshift relation but also the growth of structure in the universe (Weinberg & Kamionkowski 2003; Francis et al. 2009; Mortonson 2009; Pace et al. 2010; Khedekar et al. 2010b; Khedekar & Majumdar 2010b; Manera & Mota 2006). Hence dark energy is expected to have an impact on observables such as cluster number counts and lensing statistics (Evrard et al. 2002). Therefore, the studies of galaxy clusters would provide a useful tool to constrain the model parameters and would help to infer the properties of dark energy by discriminating among the different dark energy models.

Although the proper way to understand the effect of dark energy in the non-linear regime of structure formation is through the N-body numerical simulations, one can also use a simpler semi-analytical methods which are in reasonable agreement with N-body simulations. One such example is the spherical collapse model (Gunn & Gott 1972) using the Press-Schechter formalism(Press & Schechter 1974). To overcome the problem of over-prediction of number of low(high) mass halos at current epoch for this model, an elliptical collapse model was later proposed by Sheth & Tormen (1999).

This paper extents the previous work by Devi & Sen (2011) by further studying the most general analytic form of halo mass function introduced by Sheth & Tormen (1999) for thawing type scalar field dark energy models with various potentials and examine how does the DE affect the abundance of CDM halos by measuring the galaxy cluster number counts. We consider both the canonical and non-canonical form of thawing dark energy models. For the completeness of the study we check the results for homogeneous as well as inhomogeneous dark energy cases. We discuss how much they deviate from the conventional ΛCDM model through the linearly extrapolated density contrast $\delta_c(z)$ at the redshift of collapse, the number density of halo mass at some particular redshifts of collapse and also through the total cluster number counts.

In a recent paper Campanelli et al. (2011) have studied the constraints on different dark energy models through cluster number counts. They assumed the CPL parametrization (Linder 2003; Chevallier & Polarski 2001) to model different dark energy models. But it was recently shown by Gupta, Majumdar & Sen (2011) that this parametrization does not correctly represent all the thawing class of scalar field models. Moreover this parametrization is also not suitable for thawing scalar fields with non canonical kinetic term.

The structure of the paper is as follows: in section 2, we introduce the thawing dark energy models for both canonical and non-canonical kinetic term. We discuss the background evolution for such fields considering the difference type of potentials e.i. $V = \phi$, $V = \phi^2$, $V = e^{\phi}$ and $V = \phi^{-2}$ and also PNGB type. In section 3, we sketch the derivation of the equations to calculate the linearly extrapolated density contrast, $\delta_c(z)$, at the collapsed redshift. Then, we describe the halos mass function introduced by Sheth & Tormen (1999) and calculate the number density and the total cluster number counts for our DE models. In section 4, we discuss the deviation in the cluster abundance of dark energy models we considered from that of ΛCDM model and finally draw conclusion in section 5.

2 BACKGROUND EVOLUTION

In what follows, we consider a flat, homogeneous and isotropic background universe driven by non-relativistic matter and dark energy of thawing type, i.e. $\Omega_\phi + \Omega_m = 1$. These thawing type dark energy models are characterized by the fact that in the early universe the scalar field is frozen by very large Hubble damping and the scalar field starts evolving slowly down its potential at the later time. So, the equation of state, $w(a) = p_\phi/\rho_\phi$ initially starts with $w = -1$ and slowly departs from it in the later time. We consider both ordinary scalar field with canonical kinetic term as well as tachyon type scalar field having Born-Infeld type kinectic term which are minimally coupled to the gravity sector (Sen 2002a,b; Garousi 2000; Kluson 2000). The equation of motions for the canonical scalar field and the tachyon field are given by

$$\ddot{\phi} + 3H\phi + dV/d\phi = 0 \tag{1}$$

and

$$\ddot{\phi} + 3H\dot{\phi}(1 - \dot{\phi}^2) + \frac{dV/d\phi}{V}(1 - \dot{\phi}^2) = 0 \tag{2}$$

respectively, where dot represents the differentiation w. r. t the cosmic time t and the Hubble parameter, H is defined as

$$H^2 = \left(\frac{\dot{a}}{a}\right)^2 = \frac{8\pi G}{3}(\rho_m + \rho_\phi). \tag{3}$$

Here $a(t)$ is the scale factor, $\rho_m = \rho_{m0}a^{-3}$ is the background matter density and $\rho_\phi = \rho_{\phi 0}f(a)$ represents the dark energy density with

$$f(a) = \exp\left[3\int_a^1 \left(\frac{1 + w(u)}{u}\right) \mathrm{d}u\right]. \tag{4}$$

Defining new variables $\lambda = -\frac{1}{V}\frac{dV}{d\phi}$ and $\Gamma \equiv V\frac{d^2V}{d\phi^2} / \left(\frac{dV}{d\phi}\right)^2$, one can form an autonomous system of equations involving two observable parameters Ω_ϕ and $\gamma = (1 + w)$ together with the parameter λ. For the canonical scalar field, it is given as

$$\begin{aligned}
\gamma' &= -3\gamma(2 - \gamma) + \lambda(2 - \gamma)\sqrt{3\gamma\Omega_\phi}, && (5)\\
\Omega'_\phi &= 3(1 - \gamma)\Omega_\phi(1 - \Omega_\phi), && (6)\\
\lambda' &= -\sqrt{3}\lambda^2(\Gamma - 1)\sqrt{\gamma\Omega_\phi}. && (7)
\end{aligned}$$

For the detail derivations see the reference (Scherrer & Sen 2008a). Here the prime denotes the

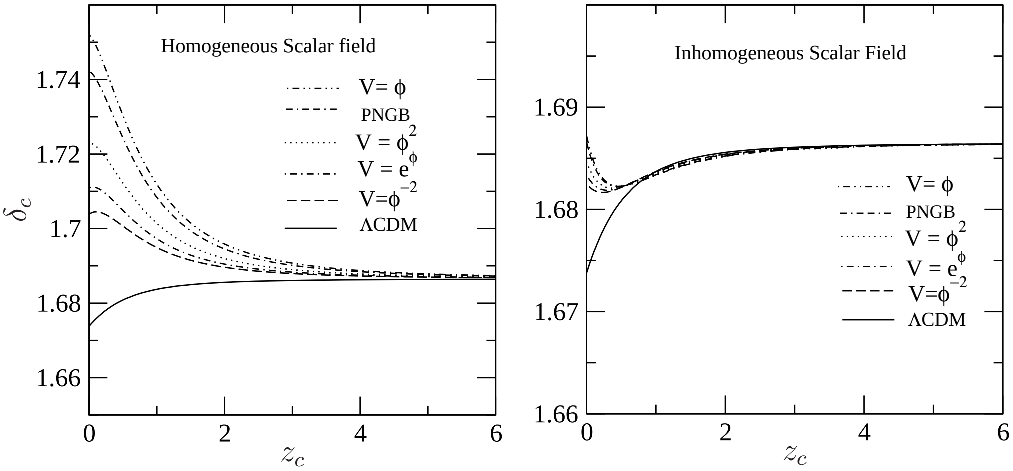

Figure 1. The redshift evolution of the linear density contrast, δ_c at the redshift of collapse for the canonical scalar field model with various potentials for $\Omega_{m0} = 0.25$. *Left panel*: Homogeneous dark energy models. *Right panel*: Inhomogeneous dark energy models. In all panels, the different potentials $V(\phi) = \phi, \phi^2, e^{\phi}$ and ϕ^{-2} are represented by different line types along with PNGB model. The ΛCDM case (black solid curve) is plotted for reference. At high redshift, all the models asymptotically approach to Einstein-de Sitter limit.

derivative with respect to ln$a$. We solve this system of equations numerically for various potentials providing the initial conditions for γ and λ as $\gamma = 0$, $\lambda_i = 1$. As discuss in Scherrer & Sen (2008a), one can easily see that smaller the value of λ_i, more the scalar field evolution similar to that of cosmological constant Λ. To check for the maximum deviation from the cosmological constant Λ, we set $\lambda_i = 1$. For Ω_ϕ we choose its initial value in such away so that to get required value at present. The difference types of potential we considered are $V = \phi$, $V = \phi^2$, $V = e^{\phi}$ and $V = \phi^{-2}$ and they correspond to $\Gamma = 0$, $\frac{1}{2}$, 1 and $\frac{3}{2}$ respectively. We also considered the Pseudo-Nambu Goldstone Boson model (PNGB) (Frieman et al. 1995) which has been characterized by the potential:

$$V(\phi) = m^4[\cos(\phi/f) + 1] \tag{8}$$

with $f = 1$. Similar for thawing tachyon field models, the autonomous system of equations is given by

$$\gamma' = -6\gamma(1-\gamma) + 2\sqrt{3\gamma\Omega_\phi}\lambda(1-\gamma)^{\frac{5}{4}} \tag{9}$$

$$\Omega'_\phi = 3\Omega_\phi(1-\gamma)(1-\Omega_\phi) \tag{10}$$

$$\lambda' = -\sqrt{3\gamma\Omega_\phi}\lambda^2(1-\gamma)^{\frac{1}{4}}(\Gamma - \frac{3}{2}) \tag{11}$$

where $\Gamma = V\frac{\frac{d^2V}{d\phi^2}}{\frac{dV}{d\phi}}$. Here also we set the initial conditions similarly as canonical scalar field case and consider the power law potentials mentioned above. For the detail calculations see the references (Scherrer & Sen 2008a,b; Ali et al. 2009).

3 HALO MASS FUNCTION

The studies of the mass function of collapsed objects like clusters of galaxies can be used to constrain the cosmological models and can help to infer the properties of dark energy. In what follows we calculate the halo mass function for the DE models considered in this paper.

3.1 Spherical collapse

As our interests lie in finding the halo-mass of CDM matter in presence of thawing dark energy, we need to study the perturbation of matter inhomogeneity in order to calculate the linear density contrast at the time of collapse. We consider a spherical region of radius $r(t)$ evolving in a cosmologically expanding background. The dynamics of this spherical region is essentially governed by the Raychaudury equation,

$$\frac{\ddot{r}}{r} = -4\pi G\left[\left(w(r) + \frac{1}{3}\right)\rho_{\phi cl} + \frac{1}{3}\rho_{mcl}\right] \tag{12}$$

where $\rho_{\phi cl}$ and ρ_{mcl} are the density of scalar field and density of the matter inside the cluster respectively. It is easier to solve the equations after normalizing at the turn around point, so we define new variables:

$$x = \frac{a}{a_t} \text{ and } y = \frac{r}{r_t}. \tag{13}$$

Subscript "t" denotes the turn around time. Now, the equations of background evolution and that of perturbation reduce to

$$\dot{x}^2 = {H_t}^2\Omega_{m,t}[\Omega_m(x)x]^{-1} \tag{14}$$

and

$$\ddot{y} = -\frac{H_{\rm t}^2\Omega_{\rm m,t}}{2}\left[\frac{\zeta}{y^2} + \nu y I(x,y)\right] \tag{15}$$

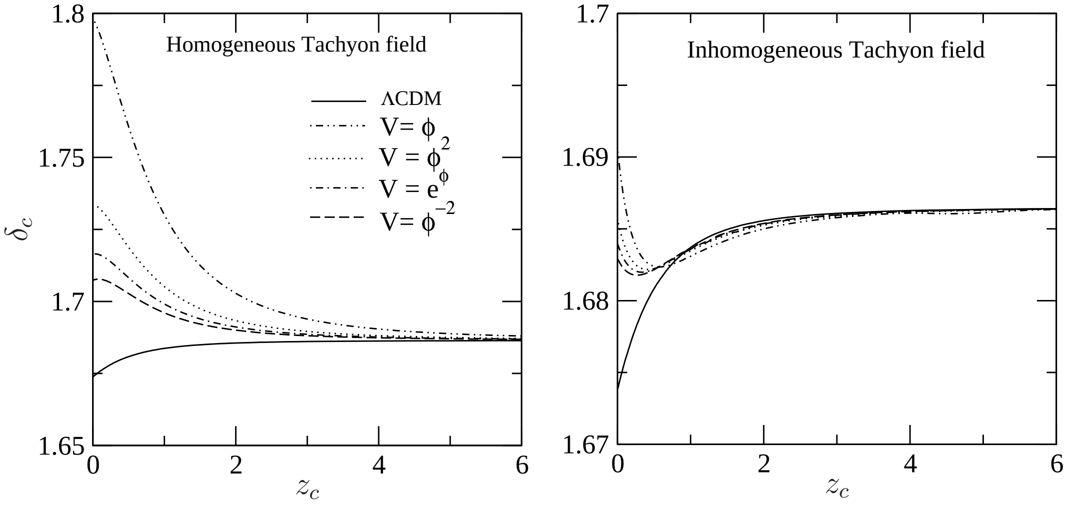

Figure 2. The redshift evolution of the linear density contrast, δ_c at the redshift of collapse for the tachyon scalar field models with various potentials for $\Omega_{m0} = 0.25$. The different potentials are represented by different line types. *Left panel*: Homogeneous dark energy models. *Right panel*: Inhomogeneous dark energy models. In all panels, the ΛCDM case (black solid line) is plotted for reference. At high redshift, all the models asymptotically approach to EDS limit.

where

$$I(x,y) = \begin{cases} [1+3w(r(y))]\,\frac{f(r(y))}{f(a_t)} & \text{Clustered DE} \\ [1+3w(x)]\,f(x) & \text{Homogeneous DE} \end{cases} \tag{16}$$

(for $I(x,y)$ see reference (Basilakos & Voglis 2007))with

$$\nu = \frac{\rho_{\phi,\mathrm{t}}}{\rho_{\mathrm{m,t}}} = \frac{1-\Omega_{\mathrm{m,t}}}{\Omega_{\mathrm{m,t}}}. \tag{17}$$

Here ζ represents the matter density contrast at turnaround which is defined as

$$\zeta \equiv \frac{\rho_{mcl,t}}{\rho_{m,t}} = \left(\frac{R_t}{a_t}\right)^{-3}. \tag{18}$$

The function $r(y)$ is given by $r(y) = r_{\mathrm{t}}y = \zeta^{-1/3}a_{\mathrm{t}}y$ and $\Omega_m(x)$ by

$$\Omega_{\mathrm{m}}(x) = \frac{1}{1+\nu x^3 f(x)}. \tag{19}$$

In addition, the linear density contrast δ obeys the equation:

$$\ddot{\delta} + 2\frac{\dot{a}}{a}\dot{\delta} = 4\pi G\rho_m\delta = \frac{3}{2}H_0^2\Omega_{m0}a^{-3}\delta. \tag{20}$$

We calculate the linear over density "δ_c" at the epoch when the spherical region described by equation (12) collapses to a point, $t(z_c) = 2t(z_t)$ by solving equation (20). For the initial condition $\delta_i = \left(\frac{\rho_{mcl}}{\rho_m} - 1\right)_{a\to 0}$, we write

$$\left[\frac{r}{a}\right]_{a\to 0} = \left[\zeta^{-1/3}\frac{y}{x}\right]_{x\to 0} = (1-\beta a_t x) \tag{21}$$

so,

$$\frac{dy_{x\to 0}}{dx} = \zeta^{1/3}(1-\beta a_t x). \tag{22}$$

Here β is the constant term which can be found by solving equations (14) and (15) after substituting (21) and (22). We neglect the higher order terms in x. For our case the initial conditions on δ_i are found out as

$$\delta_i = \begin{cases} \left[\zeta^{1/3} + \zeta^{-2/3}\nu\frac{f(r(1))}{f(a_t)}\right]\frac{a_i}{a_t} & \text{Clustered DE} \\ \left[\zeta^{1/3} + \zeta^{-2/3}\nu f(1)\right]\frac{a_i}{a_t} & \text{Homogeneous DE} \end{cases} \tag{23}$$

As we are dealing with second-order equations, two initial values are required, one for the initial over-density δ_i and other is the initial rate of evolution, $\delta_i^{'}$. $\delta_i^{'}$ is generally set to $\delta_i^{'} = 10^{-5}$. But we set $\delta_i^{'} = 0$ as the result does not change considerably. a_i is set at the matter-radiation equality epoch.

3.2 Number counts

With the indication from observations that individual galaxies and cluster of galaxies are embedded in extended halos of dark matter, the abundance of CDM halos have been studied widely. Theoretically, Press and Schetcher were the first to describe the abundance of these CDM halos as a function of their mass with the assumption that the fraction of the volume of the universe that has collapsed into objects of mass M at a redshift z follows a Gaussian distribution. The comoving number density of clusters which have collapsed (i.e., virialized) at certain red-shift z and have masses in the range $M \sim M + dM$ can be expressed as:

$$\frac{dn(M,z)}{dM} = -\frac{\rho_{m0}}{M}\frac{d\ln\sigma(M,z)}{dM}f(\sigma(z)) \tag{24}$$

where $f(\sigma(z))$ is defined as mass function. The standard Press-shechter mass function is of the form :

$$f(\sigma;PS) = \sqrt{\frac{2}{\pi}}\frac{\delta_c(z)}{\sigma(M,z)}\exp\left[-\frac{\delta_c^2(z)}{2\sigma^2(M,z)}\right]. \tag{25}$$

Although it provides a good general representation of the observed distribution of clusters, due to the discrepancy

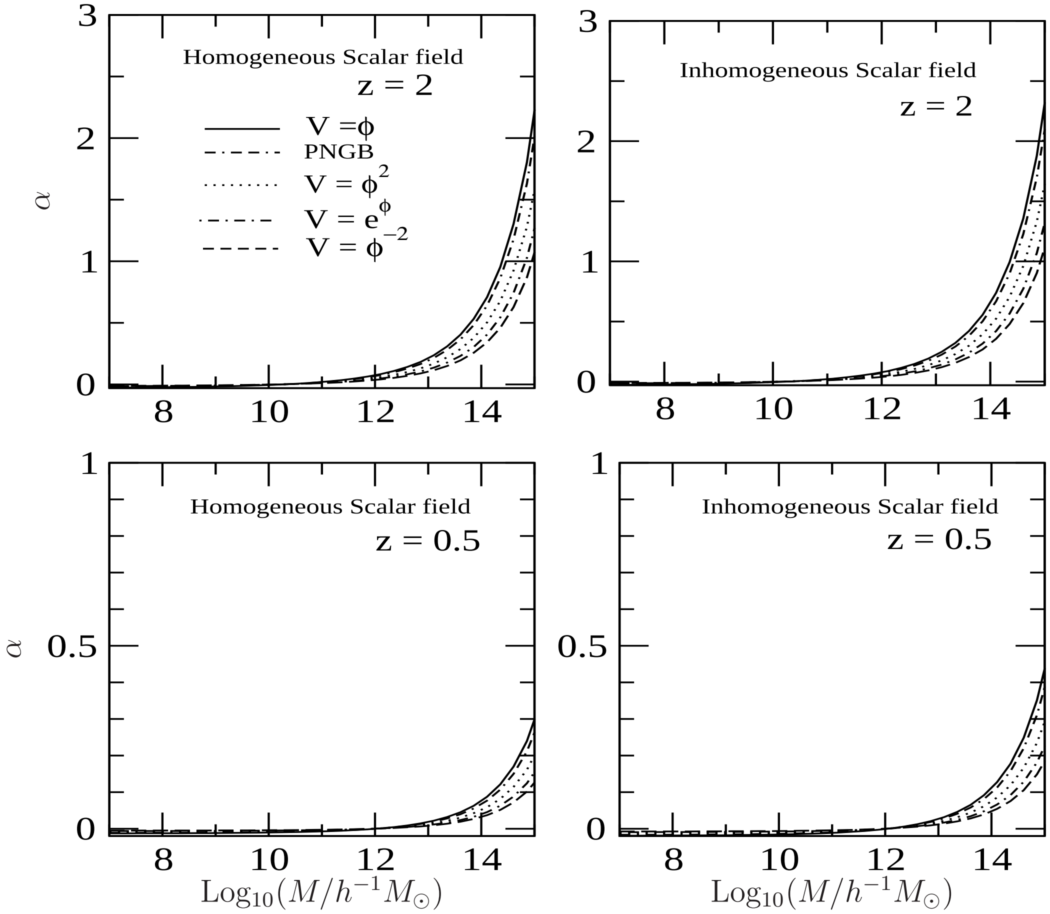

Figure 3. A comparison between the comoving number density of CDM halos for the different thawing scalar field models with that of ΛCDM model by defining a parameter, α in equation 32. *Upper panels*: Homogeneous and inhomogeneous dark energy models at redshift, $z = 2$ in the left and right panels respectively. *Lower panels*: Homogeneous and inhomogeneous dark energy models at redshift, $z = 0.5$ in the left and right panels respectively. In all panels, the various potentials are indicated by different line types. $\Omega_{m0} = 0.25$.

of over-prediction (under-prediction) of the number of low (high) mass halos at the current epoch, Sheth & Tormen (1999) introduced an ellipsoidal model of the collapse of perturbations. This Sheth-Torman mass function gives better fits to simulated mass function by reducing this discrepancy substantially. It has the form:

$$f(\sigma;ST) = A\sqrt{\frac{2a}{\pi}}\left[1+\left(\frac{\sigma^2}{a\delta_c^2(z)}\right)^p\right]\frac{\delta_c(z)}{\sigma}\exp\left[-\frac{\delta_c^2(z)}{2\sigma^2}\right] \tag{26}$$

where there contains three parameters A, a and p which we set into $A = 0.322, a = 0.707$ and $p = 0.3$ for all the models we considered. The Press-Shechter case is recovered for $a = 1$ and $p = 0$.

The dispersion of the density field on a given comoving scale R, containing mass $M = 4\pi\rho_{m0}R(M)^3/3$, is given by

$$\sigma^2(R) = \frac{D(a)}{2\pi^2}\int_0^\infty k^3P(k)W^2(kR)\frac{dk}{k} \tag{27}$$

where the quantity $P(k)$ is the power spectrum of density fluctuations extrapolated to $z = 0$ according to linear theory and $W(kR)$ is the top-hat window function;

$$W(kR) = 3\left(\frac{sin(kR)}{(kR)^3} - \frac{cos(kR)}{(kR)^2}\right) \tag{28}$$

$D(a)$ represents the growth function of linear perturbation theory and can be found from equation(20)(see fig.4 in Schaefer & Koyama (2004)). We normalize the growth function such that $D(a) = 1$ at the present epoch.

Assuming that the baryon density parameter $\Omega_{B0} \ll \Omega_{CDM,0}$, the CDM power spectrum can be approximated by $P(k) \propto kT^2(k)$ and we use the transfer function, $T(k)$ introduced by Eisenstein and Hu (Eisenstein & Hu 1998a).

The normalization of the power spectrum is often expressed in terms of σ_8, the rms fluctuation today at a scale of 8 h^{-1}Mpc. In our case, using WMAP-7 data (Komatsu et al. 2011) we normalise the power spectrum by setting $\sigma_8(\Lambda CDM) = 0.80$.

While calculating the halo mass function, we set the other cosmological parameters as $\Omega_{m0} = 0.25,\ \Omega_{\phi0} = 0.75,\ h = 0.72,\ \Omega_{B0} = 0.0456$ and $n_s = 1$.

We calculate $dn/d\log M$ as a function of M at a partic-

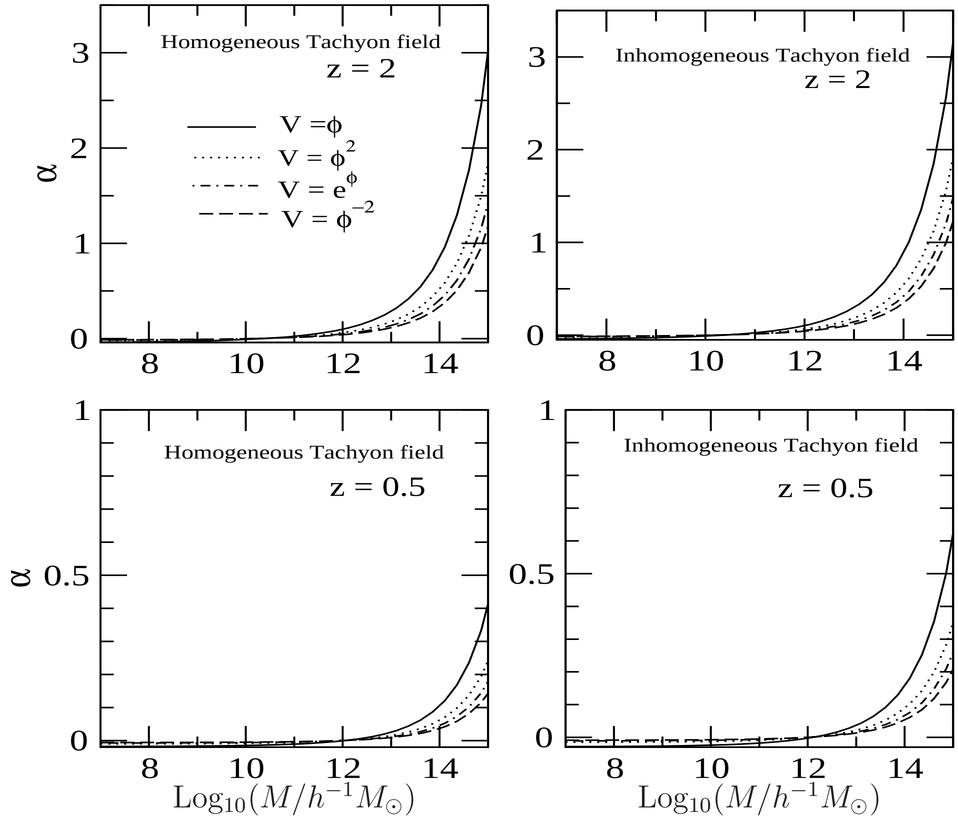

Figure 4. Same as figure 3. for the tachyon field dark energy models. The various potentials are indicated by different line types.

ular z ($z = 0.5$ and 2) for both the cases of thawing models with various potentials and shown in figures (3) and (4).

The number of clusters in a redshift interval dz, above a given minimum(threshold) $M = M_{min}$ is obtained from $dn(M, z)/dM$:

$$\frac{dN}{dz}(M > M_{min}) = f_{sky}\frac{dV(z)}{dz}\int_{M_{min}}^{\infty} dM\frac{dn}{dM}(M, z) \quad (29)$$

where f_{sky} is the fraction of the sky being observed and the comoving volume element is given by

$$\frac{dV}{dz} = 4\pi r^2(z)\frac{dr}{dz}. \quad (30)$$

$r(z)$ is the comoving radial distance out to redshift z:

$$r(z) = \frac{c}{H_0}\int_0^z \frac{dz^{'}}{H(z^{'})}, \quad (31)$$

where $H(z)$ is the Hubble parameter. For numerical computation, the upper limit of integration in equation (29) is replaced by some finite mass value M_{max}. The comoving volume element is required since the redshift evolution of a physical volume in space is model dependent, i.e, depending on the form of potentials.

4 RESULTS AND DISCUSSION

In this section, we discuss the results for the linear overdensity contrast, the number density of CDM halos and the total clusters number counts for the models we introduced, keeping the ΛCDM model as a reference since the ΛCDM model is currently the simplest model, fitting all available observational data despite of its conceptual problems.

One of our results are shown in Fig.1 where we show the linear density contrast, δ_c, as a function of collapsed redshift for both homogeneous (left panel) and inhomogeneous (right panel) scalar field models with various potentials. The similar behavior is being shown for the case of tachyon field in figure 2. From figure 1 and 2, it can be seen that the linear density contrast δ_c at $z = 0$ has a significant deviation from ΛCDM case for homogeneous dark energy models. These deviations are comparatively smaller in case of inhomogeneous dark energy. This is true for both ordinary scalar field as well as tachyon type scalar field. One may expect this type of behavior. For homogeneous case, the equation of state of dark energy is greater than $w = -1$ (we are not considering Phantom models). Hence the repulsive effect of dark energy in the background evolution is lesser than the ΛCDM case. This results larger linear density contrast for homogeneous dark energy. However, for inhomogeneous case, there is an extra

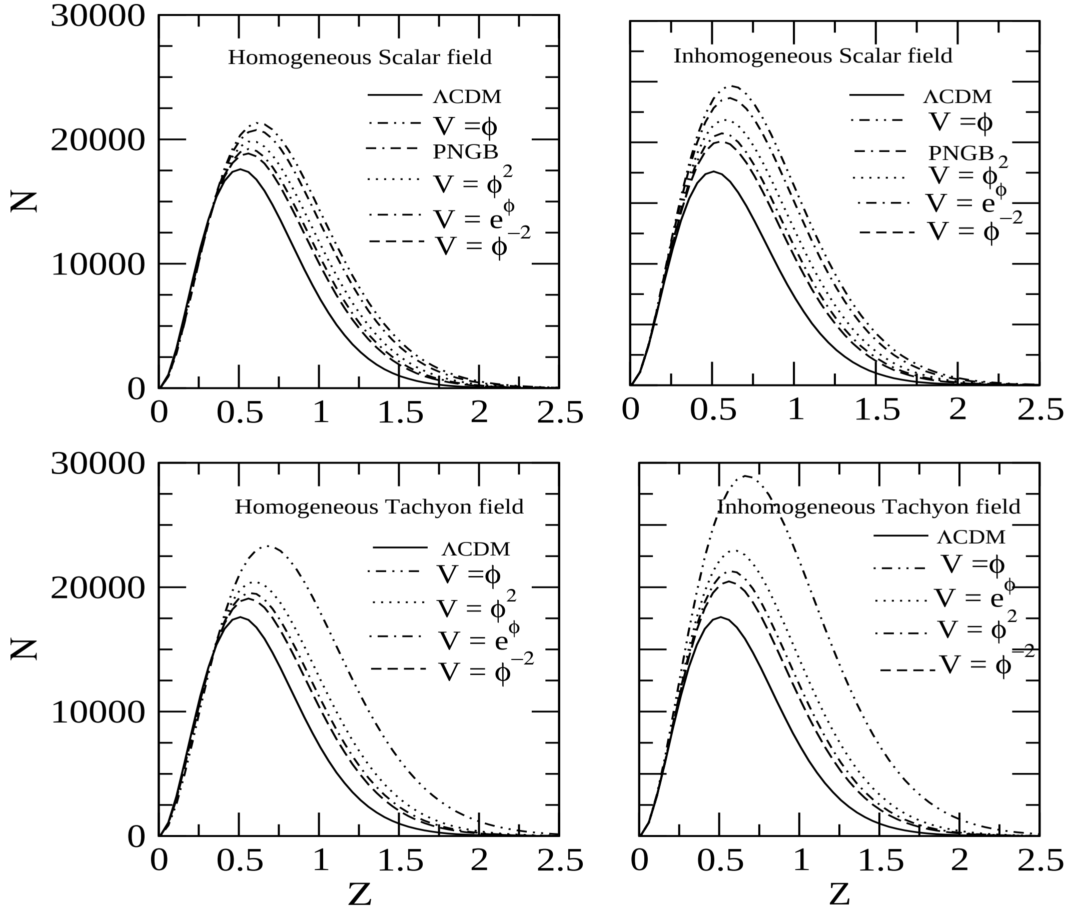

Figure 5. The total number counts N as a function of redshift of Z, integrated over mass (from $M_{min} = 2 * 10^{14} M_{\odot}$) for a survey area of 10, 000 square degree. All the models are normalised to the same number density of haloes today. *Upper panel*: The canonical scalar field models with homogeneous (left) and inhomogeneous dark energy cases (right).*Lower panels*: The tachyon scalar field models with homogeneous and inhomogeneous dark energy cases in the left and right panels respectively. The different potentials correspond to the different line types. The concordance ΛCDM model (black solid line) is also plotted for comparison. $\Omega_{m0} = 0.25$.

repulsive effect inside the cluster due to inhomogeneous dark energy. This reduced the linear density contrast for inhomogeneous DE and brings it closer to the ΛCDM value. At high redshift, all the models asymptotically approach to Einstein-de Sitter (EDS) limit. Among the potentials we considered, the linear potential shows the maximum deviation from the ΛCDM for both the ordinary and tachyon fields as well as for homogeneous and inhomogeneous case. This is consistent with the results earlier obtained by Devi & Sen (2011).

Next, we investigate a quantity closely related to observations, the clusters number density, $dn/d\log M$, the number of the collapsed objects per unit mass per unit volume. Since it is only depends on δ_c and on the growth factor, no appreciable differences are expected between the models studied. In order to see the significant deviation in the cluster number density for the thawing models from that of the standard ΛCDM, we define a new parameter, α such that

$$10^{\alpha} = \frac{dn/d\log M}{(dn/d\log M)_{\Lambda CDM}}. \qquad (32)$$

This parameter measures the deviation in the clusters number density of any thawing models from that of ΛCDM. Larger the value of α more it deviates from ΛCDM. The behavior of α for ordinary scalar field as well as for tachyon type field have been shown in figure (3) and (4) respectively. It can be seen from figure (3) that α value is higher for higher z i.e. the clusters number density for the object collapsing earlier have significant deviation from that of the ΛCDM. This is true for both ordinary scalar field and tachyon field in homogeneous as well as inhomogeneous DE cases. The difference between the homogeneous and inhomogeneous is prominent for the object collapsing at the later time (i.e. at redshift $z = 0.5$). Again if we look further, the tachyon field models show larger deviations from ΛCDM at all redshifts than the scalar field with canonical kinetic term. Among the potentials we considered, the linear potential again shows the maximum deviation for the tachyon dark energy models for homogeneous as well as inhomogeneous cases.

An another important quantity that can be derived from observations is the total number counts of halos CDM above a given mass in a complete survey volume. There are a number of cluster surveys ongoing or being planned in near future, e.g., PLANCK, eROSITA, WFXT which would detect a large number of clusters (Vikhlinin et al. 2009b). To obtain the mass of the clusters detected, one usually utilizes a proxy variable which can be the X-ray flux, SZE flux or richness of the cluster. The actual quantity chosen would, of course, depend on the nature of the survey. The relation between these quantities and the mass depends on the detailed cluster physics. However, for our purpose, it suffices to state that the limiting mass $M_{\rm min}(z)$ of the survey will be essentially determined by the limits on the proxy variable.

For predicting the number of clusters would be detected in a typical cluster survey we set the fraction of the sky being observed as $f_{\rm sky} = 0.2424$, which corresponds to a survey area of 10,000 deg^2, appropriate for surveys like eROSITA and WFXT. The value of $M_{\rm min}$ would depend on the flux limit of the survey and hence it will be a function of z. For simplicity, we choose a constant value $M_{\rm min} = 2 \times 10^{14} h^{-1} M_{\odot}$, which roughly corresponds to a flux limit (in the energy band 0.5–2 keV) of $\sim 10^{-14}$ erg cm^{-2} s^{-1}. We show the calculated value of the total number counts of CDM halos as the function of redshift in the Figs (5) for all the models we considered. We discuss the results below.

It is clear that there exists significant difference in the number counts between different DE models considered. The difference is most significant around $z \sim 0.5 - 1$. To take a specific example, we see from the top-left panel that the difference in number counts between ΛCDM and $V = \phi$ homogeneous scalar field model is ~ 2000 at $z \sim 0.7$. This difference is significantly larger than the statistical uncertainties (which would be ~ 100 for the type of surveys we are considering), and hence can be used for discriminating between different models. The same conclusions can be drawn from other panels as well.

We should mention that discriminating between different DE models would be limited by our ignorance of other cosmological parameters like Ω_m, σ_8, n_s. A proper analysis of how to constrain the models would involve error estimates of the parameters with a combination of different observational data sets, e.g., cluster counts, CMBR, BAO etc. This is beyond the scope of this paper and would be attempted separately in future.

5 CONCLUSION

To summarize, we investigate the cluster abundances in cosmological scenario where the universe is dominated by the thawing class of scalar dark energy. We consider both the ordinary scalar field with canonical kinetic term as well as well as tachyon field with DBI form of kinetic energy. Moreover, we consider a variety of potentials that can give rise to suitable cosmological scenario different from concordance ΛCDM model. To study the formation of collapsed structures, we consider homogeneous dark energy as well as dark energy scenario where dark energy takes part in the virialisation process. We consider the Press-Schetcher formalism modified by Sheth & Tormen (1999) to calculate the mass function. Subsequently, we show that there exists significant difference in the number counts between different dark energy models and the concordance ΛCDM model. Given the fact that a large number of cluster surveys are currently ongoing as well as a number of future surveys are being planned, this can be a smoking gun to distinguish different dark energy models from ΛCDM. Our present work is one preliminary step towards that direction. This work can be extended to freezing class of scalar field models as well as for models with non minimally coupled scalar fields. This will be our future aim.

6 ACKNOWLEDGEMENT

A. A. SEN acknowledges the financial support provided by the SERC, DST, Govt. of India through the research grant (DST-SR/S2/HEP-043/2009. NC Devi acknowledges the financial support provided by CSIR, Govt. of India. NC Devi also acknowledges the Harish-Chandra Research Institute, Allahabad, India for hospitality provided during her visit where part of the work has been done.

REFERENCES

Abramo L. R., Batista R. C., Liberato L. & Rosenfeld R., 2007 JCAP, 11, 012
Ali A., Sami M., &, Sen A. A., 2009, Phys. Rev. D, 79, 123501
Baccigalupi C. & Acquaviva V., 2006, [astro-ph/0606069]
Bahcall N. A., et al., 2003, ApJ., 585, 182
Baldi M., Pettorino V., Robbers G. & Springel V., 2008, [arXiv:0812.3901]
Bartelmann M., Huss A., Colberg J. M., Jenkins A., & Pearce F. R., 1998, Astron. Astrophys., 330, 1
Basilakos S. & Voglis N., 2007, MNRAS, 374, 269,
Bharadwaj S., Sethi S. K. & Saini T. D., 2009, Phys. Rev. D, 79, 083538
Borgani S., et al., 2001, ApJ., 561, 13
Caldwell R. R. & Linder E. V., 2005, Phys. Rev. Lett., 95, 141301
Campanelli L., Fogli G. L., Kahniashvili T., Marrone A. & Bharat Ratra, 2011, [arXiv:1110.2310]
Carroll S. M., 2001, Living Rev. Rel., 4, 1
Chevallier M. & Polarski D., 2011 Int. J. Mod. Phys. D, 10, 213
Cole S., et al, 2005, MNRAS, 362, 505
Corasaniti P .S., Giannantonio T. & Melchiorri A., 2005, Phys. Rev. D, 71, 123521
Corless V. L. & King L.J., 2009, MNRAS, 396, 315
Courtin J. et al., 2011, MNRAS, 410, 1911
Dahle H., 2006, ApJ., 653, 954
Devi N. C. & Sen A. A., 2011, MNRAS, 413, 2371
Eisenstein D. J. & Hu W., 1998a, ApJ, 496, 605
Eisenstein D. J., Hu W., Silk J. & Szalay A. S., 1998b, ApJ, 494, L1
Evrard A. E., et al., 2002, ApJ., 573, 7
Francis M. J., Lewis G. F. & Linder G. F., 2009, MNRAS, 393, L31

Frieman J. A., Hill C. T., Stebbins A. & Waga I.,1995, Phys. Rev. Lett., 75, 2077

Garousi M. R., 2000, Nuclear Phys. B, 584, 284

Gunn J. E. & Gott J. R., 1972, ApJ, 176, 1

Gupta G., Majumdar S. & Sen, A.A., (arXiv:1109.4112), to appear in MNRAS.

Horellou C. & Berge J., 2005, MNRAS, 360, 1393

Jain B. & Taylor A., 2003, Phys. Rev. Lett., 91, 141302

Kluson J., 2000, Phys. Rev. D, 62, 126003

Khedekar S., Das S. & Majumdar S., 2010a, Phys. Rev. D., 82, 1301

Khedekar, S. & Majumdar, S., 2010b, Phys. Rev. D, 82, 081301

Komatsu E., et al., 2011, Astrophys. J. Suppl. 192, 18

Kowalski M., et al., 2008, ApJ, 686, 749

Linder E. V., 2003, Phys. Rev. Lett. 90, 091301

Macci A. V., Quercellini C., Mainini R., Amendola L. & Bonometto, S. A., 2004, Phys. Rev. D, 69, 123516

Macorra A. de la., 2003, Phys. Rev. D, 67, 103511

Manera M. & Mota D. F., 2006, MNRAS, 371, 1373

Mortonson M. J., 2009, Phys. Rev. D., 80, 123504

Nunes N. J. & Mota D. F., 2006, MNRAS, 368, 751

Pace F., Waizmannm J-C. & Bartelman M., 2010, MNRAS, 406, 1865

Padmanabhan T., 2005, Curr. Sci., 88, 1057.

W. J. Percival W. J., et al., 2009, MNRAS, 401, 2331.

Pogosian L., et al., 2005, Phys. Rev. D, 72, 103519

Press W. H., Schechter P., 1974, ApJ, 187, 425

Reiprich T. H. & Bohringer H., 2002 ApJ., 567, 716,

Riess A. G., et al., 2009, ApJ, 699, 539

Sahni V. & Starobinsky A., 2000, Int. J. Mod. Phys. D, 9, 373

Schaefer B. M. & Koyama K., 2008, MNRAS, 385, 411

Scherrer R. J., &, Sen A. A., 2008a Phys. Rev. D, 77, 083515

Scherrer R. J., &, Sen A. A., 2008b Phys. Rev. D, 78, 067303

Seo H. J., Eisenstein D. J., 2005, ApJ, 598, 720

Sen A., 2002a, J. High Energy Phys., 0204, 048

Sen A., 2002b, Mod. Phys. Lett. A, 17, 1797

Sheth R. K. & Tormen G., 1999, MNRAS, 308, 119

Tauber J. A., 2005, New Cosmological Data and the values of the Fundamental Parameters, 201, 86

Vikhlinin A., et al., 2009, ApJ., 692, 1060

Vikhlinin A., et al., 2009b, [arXiv:0903.5320]

Wang L. & Steinhardt P. J., 1998, ApJ, 508, 483

Weinberg N. N. & Kamionkowski M., 2003, ApJ, 341, 251

Wen Z. L. Han , J. L. & Liu F.S., 2010, [arXiv:1004.3337]

Wintergerst N. & Pettorino V., 2010, Phys. Rev. D, 82 103516